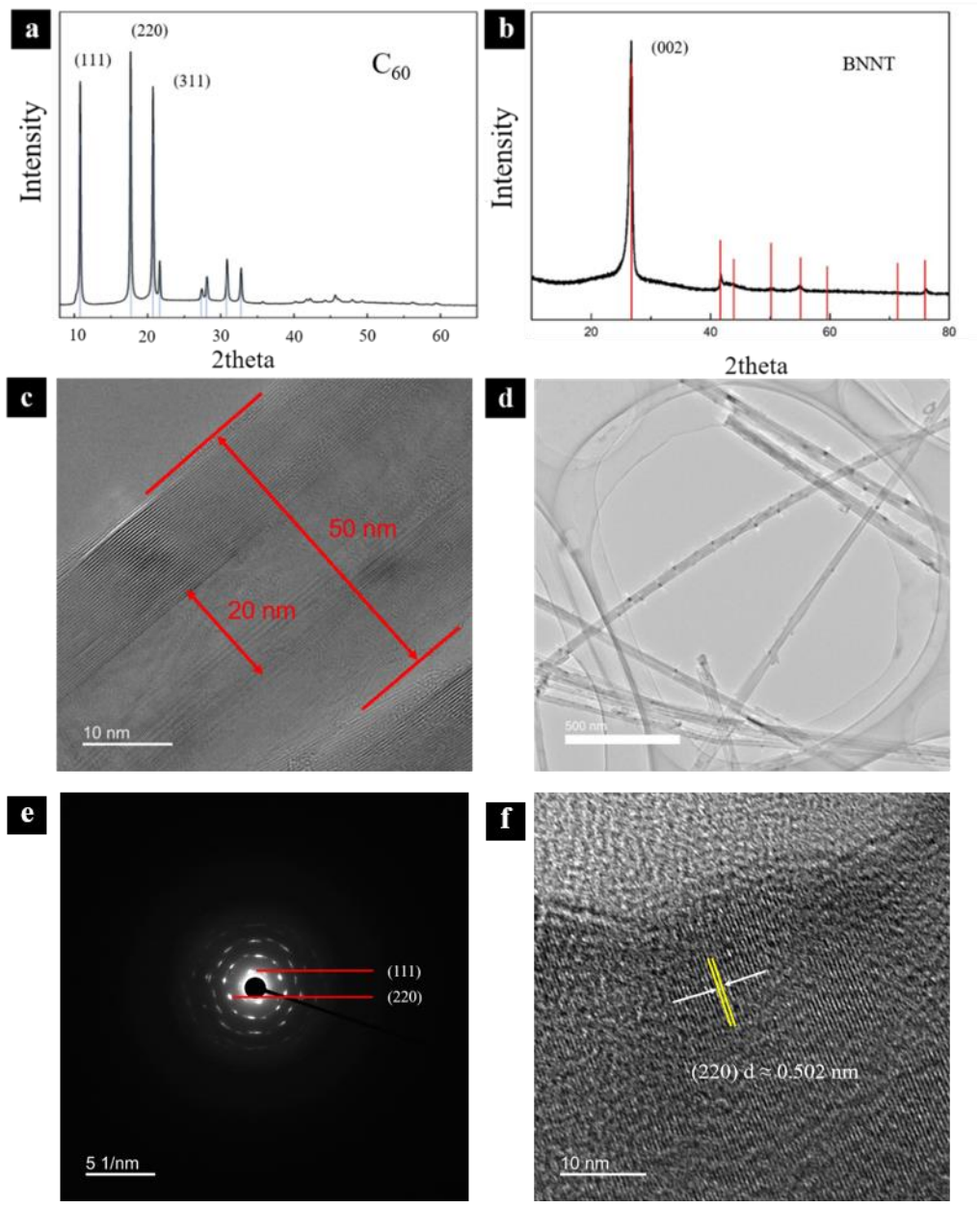

Figure S1 XRD pattern of C_{60} (a) and BNNT (b); TEM images of BNNT (c, d) and C_{60} (e, f).

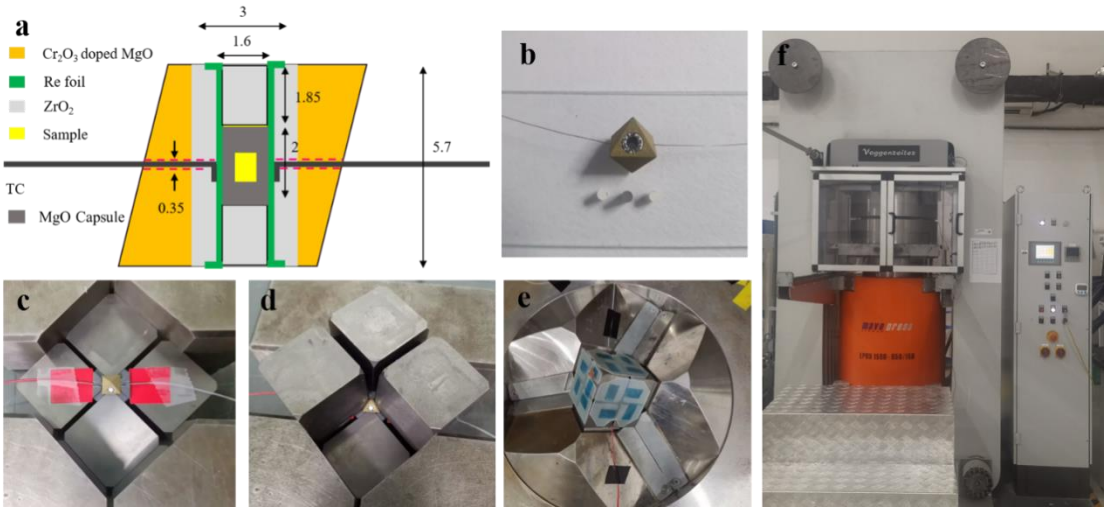

Figure S2 Schematic diagram of high pressure and high temperature experiment process.

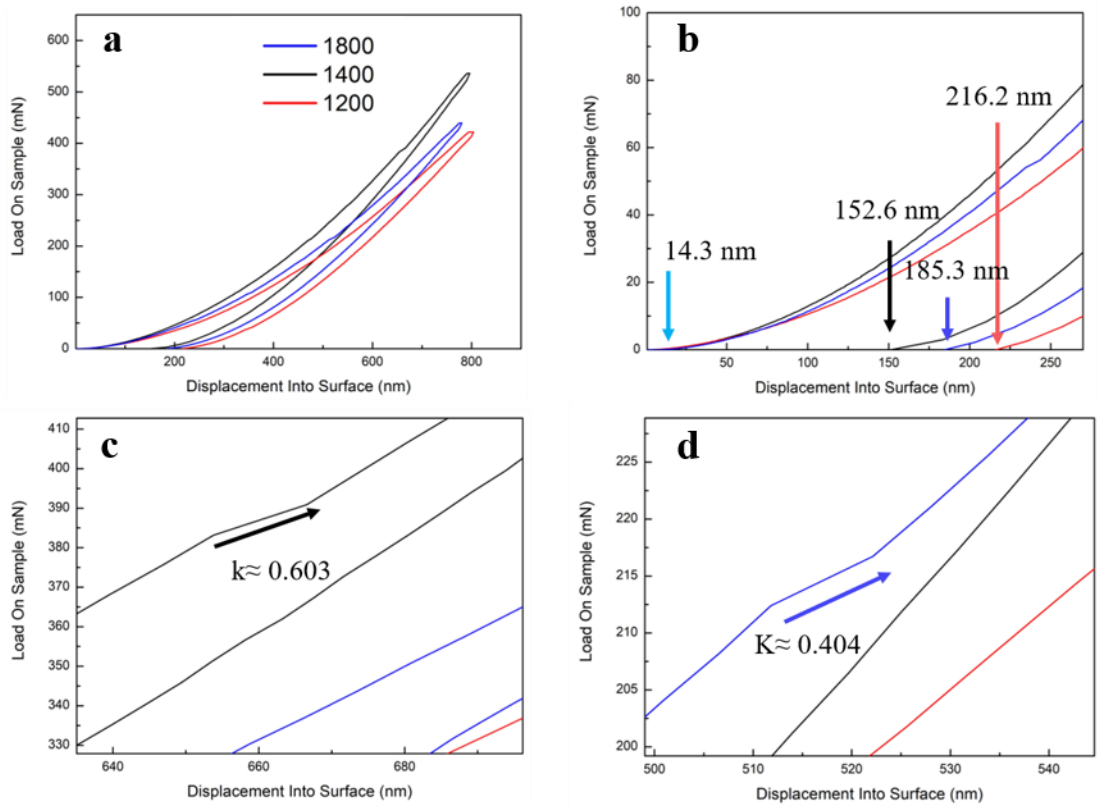

Figure S3 Applied load and indentation depth curves of different samples.

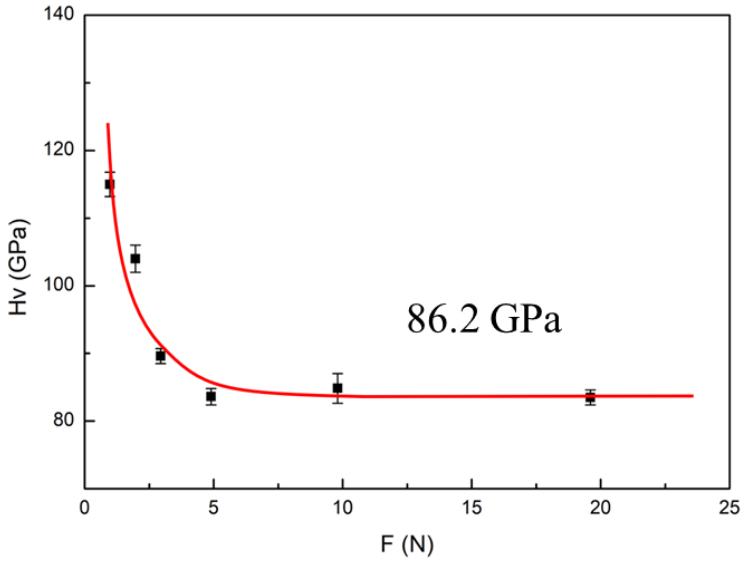

Figure S4 Hardness asymptote for the recovered sample obtained at 25 GPa 1400 ℃.

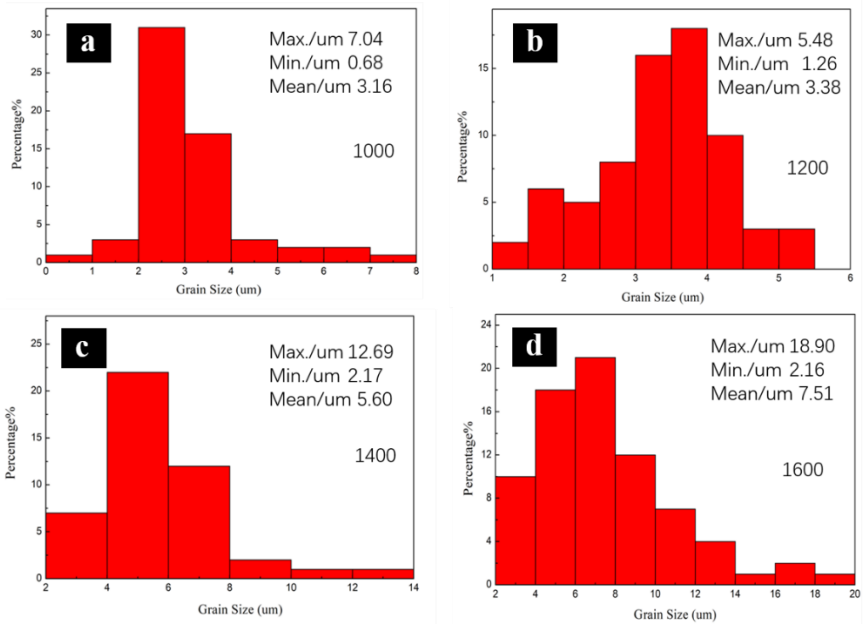

Figure S5 Average grain size of carbon in samples at different temperatures.

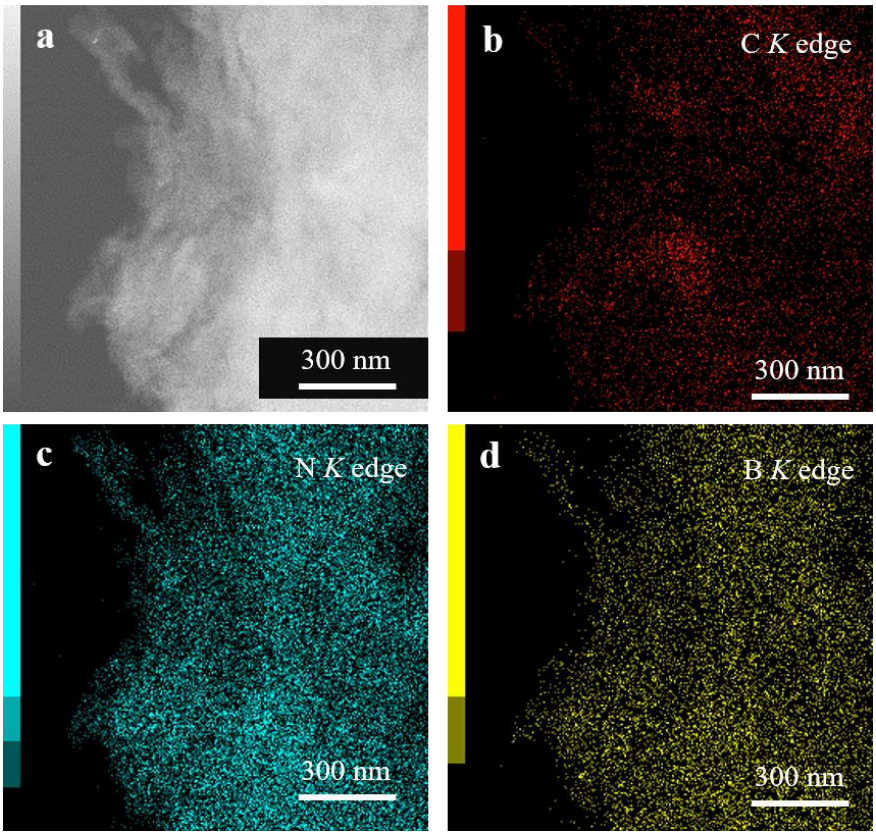

Figure S6 Elemental Mapping of the recovered sample obtained at 500 ℃

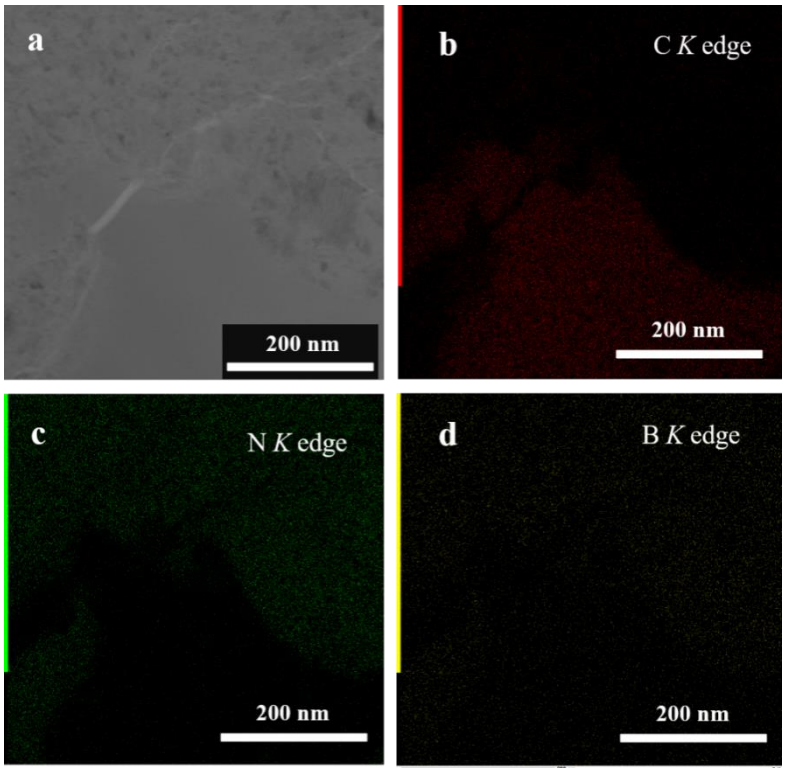

Figure S7 Elemental Mapping of the recovered sample obtained at 1200 ℃

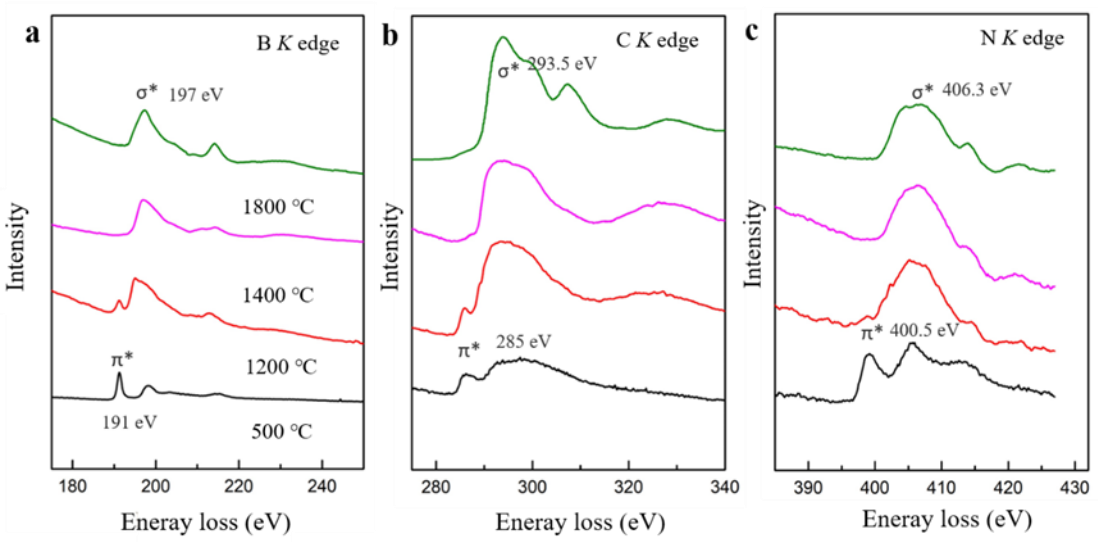

Figure S8 EELS spectra of samples obtained at different temperatures

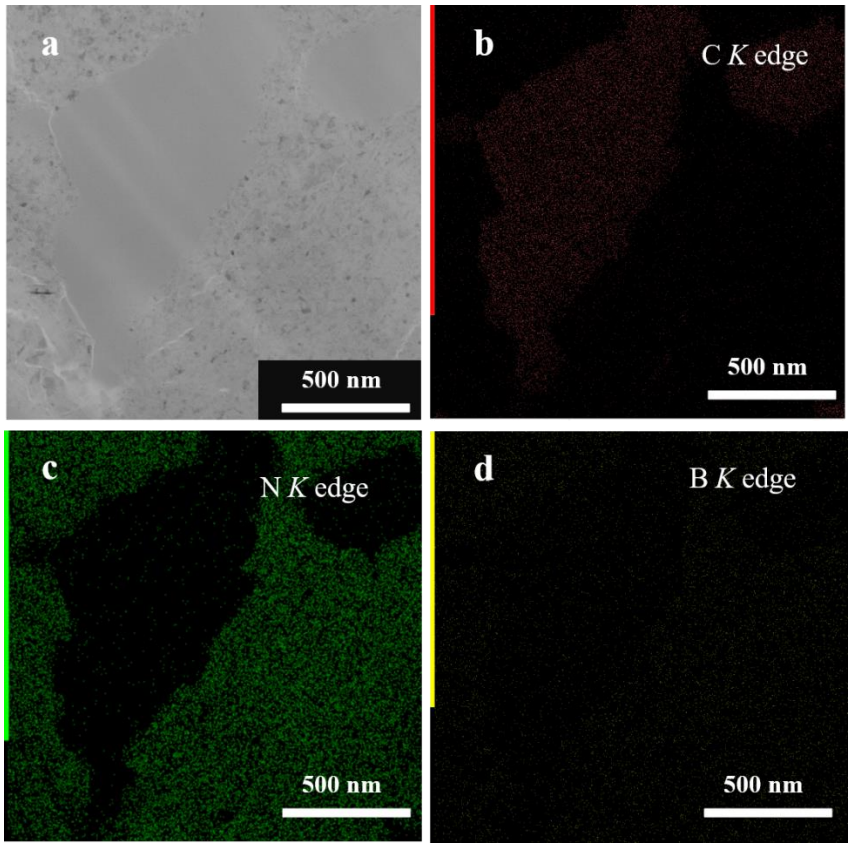

Figure S9 Elemental Mapping of the recovered sample obtained at 1400 °C 25 GPa

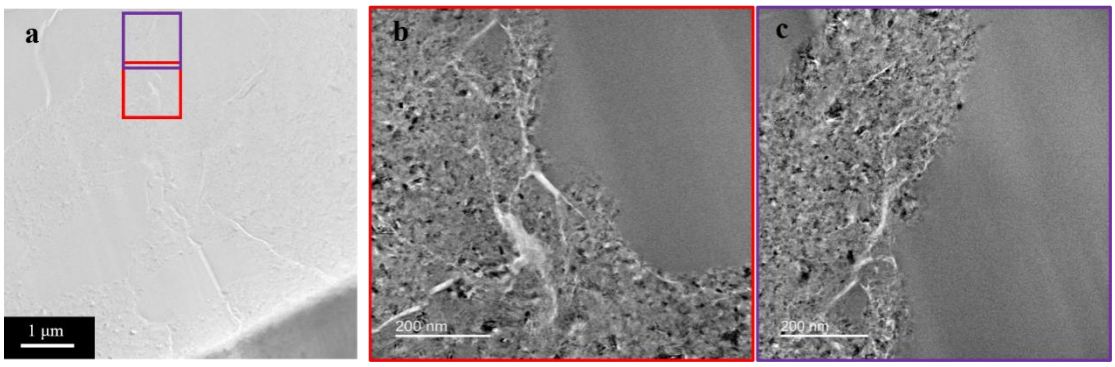

Figure S10 (a) Fracture morphology in the indentation area of the sample obtained at 25 GPa 1400 ℃; (b, c) Zooming in images of Figure a, Cracking morphology at boundaries.

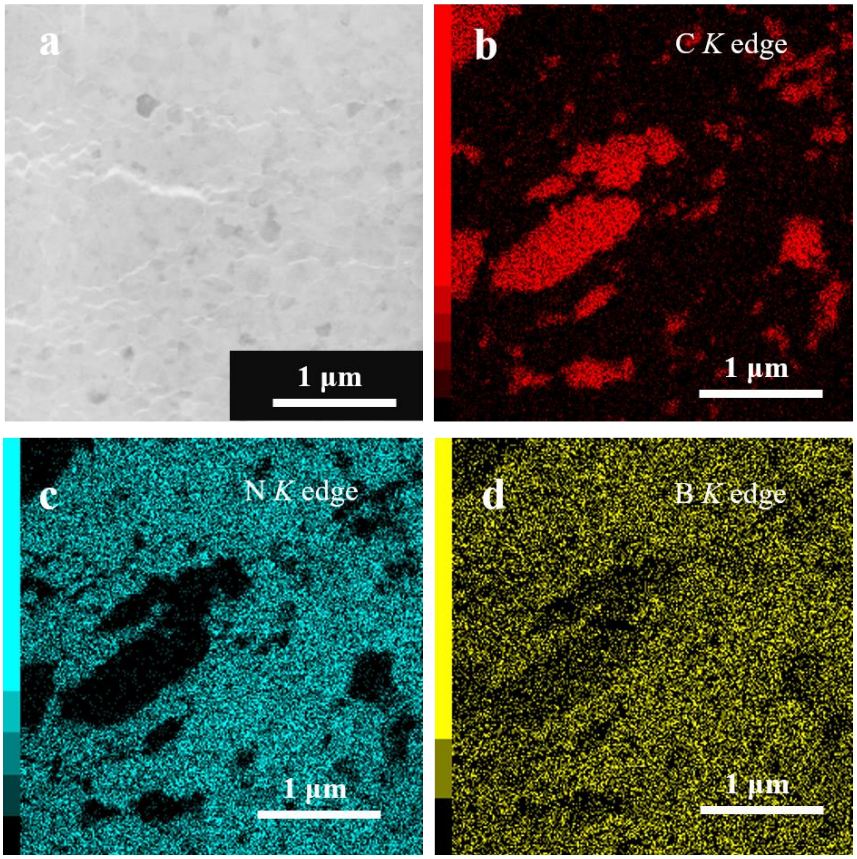

Figure S11 Elemental Mapping of the recovered sample obtained at 1800 ℃ 25 GPa

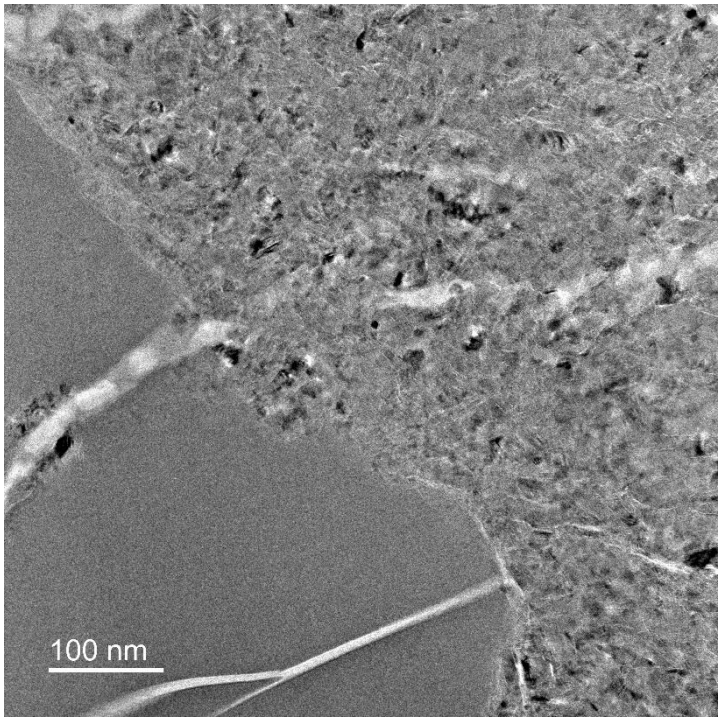

Figure S12 Morphological image of crack tip passing through amorphous diamond-like carbon of recovered sample at 25GPa 1400 ℃.

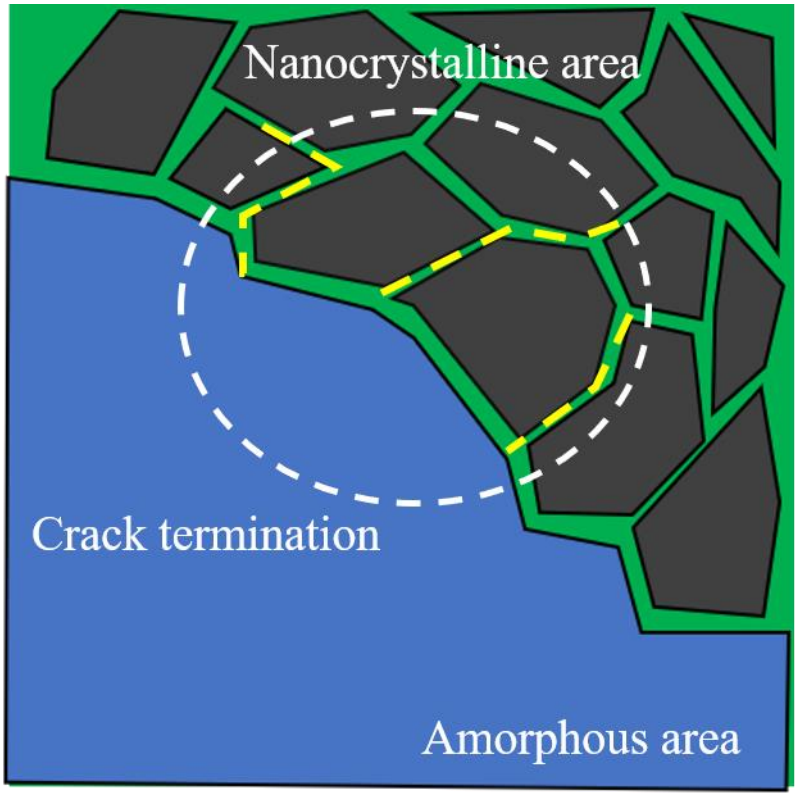

Figure S13 Schematic diagram of amorphous diamond-like carbon particles hindering the migration of crack tips.